

# Ion acceleration in "dragging field" of a light-pressure-driven piston

Liangliang Ji<sup>1,2</sup>, Alexander Pukhov<sup>1</sup>, and Baifei Shen<sup>2</sup>

<sup>1</sup>*Institut für Theoretische Physik I, Heinrich-Heine-Universität Düsseldorf, 40225 Düsseldorf, Germany and*

<sup>2</sup>*Shanghai Institute of Optics and Fine Mechanics,  
Chinese Academy of Sciences, Shanghai 201800, China*

We propose a new acceleration scheme that combines shock wave acceleration (SWA) and light pressure acceleration (LPA). When a thin foil driven by light pressure of an ultra-intense laser pulse propagates in underdense background plasma, it serves as a shock-like piston, trapping and reflecting background protons to ultra-high energies. Unlike in SWA, the piston velocity is not limited by the Mach number and can be highly relativistic. Background protons can be trapped and reflected forward by the enormous "dragging field" potential behind the piston which is not employed in LPA. Our one- and two-dimensional particle-in-cell simulations and analytical model both show that proton energies of several tens to hundreds of GeV can be obtained, while the achievable energy in simple LPA is below 10 GeV.

PACS numbers: 52.38.r, 42.65.Re, 52.27.Ny, 52.65.Rr

Laser-driven ion acceleration attracts more and more attention nowadays because of its potential to realize table-top size ion accelerators, which would greatly reduce the expense and occupying area compared to conventional accelerators. In most proposals, intense/ultra-intense laser pulses are employed to stimulate strong electrostatic fields with amplitude several magnitudes higher than that of conventional methods. These fields move at high velocities thus ions can be continually accelerated to large energy in a short distance. In Target Normal Sheath Acceleration (TNSA) [1–8], the sheath field, formed at the target back by laser heated super-thermal electrons, moves at several to tens of the ion acoustic speed. Ions co-move with the field and are accelerated to tens of MeV, while energy above hundred MeV is quite a challenge because of the weak scaling law versus laser intensity. In Light Pressure Acceleration (LPA) [9–16], electrons in the thin plasma foil are pushed inward by the laser pressure and build up an intense charge separation field, by which protons are accelerated. As the foil is driven as a whole, protons move along with the electrostatic field and are successively accelerated to energies that theoretically may reach GeV. Nevertheless, even in simulations it is difficult to overcome the ten GeV barrier for protons with LPA, since the accelerating gradient drops quickly due to the relativistic Doppler effect. As soon as the protons become relativistic, their energy grows very slowly with time ( $\sim t^{1/3}$ ).

Recently, a breakthrough in collisionless shock wave acceleration [17–22] has been reported [19]. It suggests that a multi-pulsed picosecond (ps) laser pulse can efficiently excite a collisionless shock and maintain its velocity in a density-decaying plasma target. The produced protons have much larger energy and lower energy spread than predicted by the hole-boring shock [20]. When the shock propagates like a piston, some protons are trapped and reflected to a speed determined by the energy density gradient. The exponentially decaying density profile of the

target is important for keeping the shock velocity high and constant. However, plasma itself also expands at the ion acoustic speed simultaneously. It seems inevitable that the pressure gradient will be further weakened at a later stage. This would put a limit on the final energy gain. From other side, the shock wave velocity is limited by the Mach number, which cannot be very high [21].

Generally, the shock front may be considered as a fast-moving piston carrying a strong electrostatic field. Imagine, one could free the limitation on its velocity, e.g., the shock becomes relativistic [23]. Then, the trapped and reflected protons would reach a relativistic  $\gamma$ -factor of about  $\gamma = 2\gamma_s^2$ , where  $\gamma_s$  is the relativistic factor of the shock wave. This is a way beyond the simple thermal shock wave acceleration. An intense electrostatic field moving at relativistic velocity is required. One possibility might be the plasma wakefield. It works very good for electron acceleration, however it may be not intense enough to trap protons, although there are some proposals to trap pre-accelerated protons and accelerate them further by the wakefield to very high energies [24].

We propose here that the electrostatic field of LPA can serve as the perfect relativistic piston. Its velocity is close to the light speed and the charge separation field is sufficiently high to trap background protons. In this paper, we develop an analytical model and use particle-in-cell (PIC) simulations to show that when a thin foil driven by ultra-intense circularly polarized (CP) laser pulses, with peak amplitude  $a_0 = eE_L/m_e\omega_0c$  from 50 to 200, passes through an underdense plasma region, reflected protons can achieve energies up to hundreds of GeV. Here  $e$  and  $m_e$  are fundamental charge and electron mass,  $E_L$  and  $\omega_0$  are electric field amplitude and angular frequency of the laser pulse,  $c$  is the light speed, respectively.

The expression of the accelerating field amplitude as a function of time is derived, which, together with the foil momentum equation, well describes the movement of the background protons and the trapping condition. The

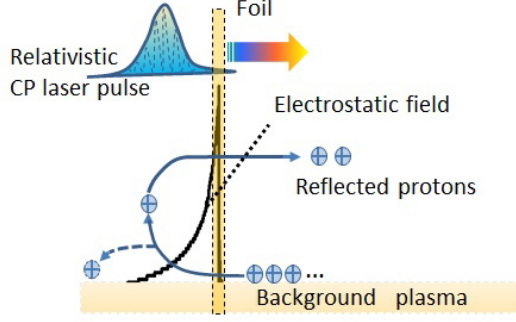


Figure 1: The electrostatic field driven by a relativistic CP laser propagates in the underdense background plasma, traps background protons and reflects them to ultra-high energy.

scaling laws indicate that the peak energy increases with  $t^{2/3}$  and  $a_0^2$ . A proof-of-principle two-dimensional (2D) simulation is also performed to show the validity of our analysis in a multi-dimensional geometry.

The mechanism is sketched in Fig. 1. As known in LPA, the laser-driven foil is accompanied by an intense charge separation field. When it propagates through the low density plasma, background protons can be continuously trapped in certain conditions. The foil plays the role of a relativistic piston. In the frame of the relativistic piston, background protons clash towards the electrostatic field at the foil velocity, then are slowed down by the field in and behind the foil and finally reflected.

In LPA, protons are accelerated by the field localized in the ultra-thin skin layer only, leaving the enormous "dragging field" (DF) unused. In our scheme, the background protons pass through the skin layer and are greatly accelerated by the DF, which contains much more electrostatic potential than the field inside the layer. As a result, the reflected protons can obtain energy a magnitude higher than foil protons in the simple LPA regime.

To demonstrate the mechanism a 1D PIC simulation is performed by the VLPL code [25]. A dense thin foil, with density of  $n_f = 150n_c$  and thickness of  $d_f = 0.57\lambda_0$ , is driven by a CP laser pulse with peak amplitude  $a_0 = 150$ , where  $n_c = m_e\omega_0^2/4\pi e^2$  is the critical density and  $\lambda_0 = 0.8\mu m$  is the laser wavelength. For simplicity, we used a trapezoidal laser pulse. Its amplitude increased linearly to the maximum in  $2T_0$  and then stayed constant ( $T_0$  is the laser period). Here the foil thickness is optimized for LPA [26]. A background plasma with density of  $n_b = 0.001n_c$  is located behind the foil. Fig. 2(a) shows distributions of the electrostatic field and momentum of background protons. The field decays quickly at first and much more slowly later. It is so intense, well beyond  $E_0 = m_e\omega_0 c/e$  even at the end of the interaction, that background protons are gradually trapped and reflected to about 70 GeV in 3mm, while protons in the

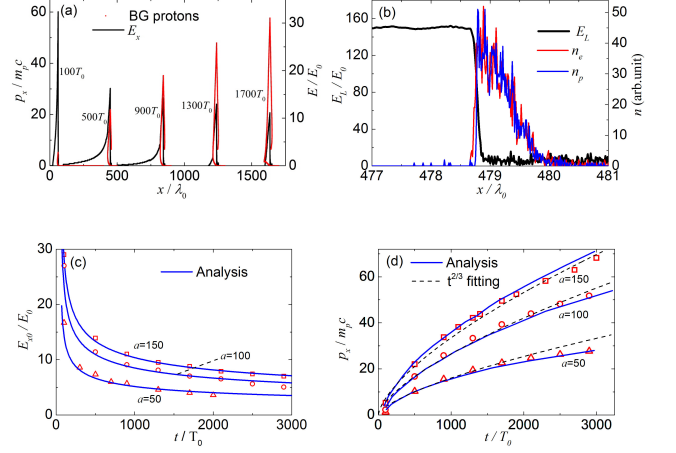


Figure 2: a) Distributions of electrostatic field (blue solid) and momentum of background (BG) protons (red dotted) at different stages with  $a_0 = 150$ ,  $n_f = 150n_c$ ,  $d_f = 0.57\lambda_0$  and  $n_b = 0.001n_c$ . b) Distributions of laser field (black solid), electron density (red solid) and proton density (blue solid) at  $t = 500T_0$ . c) Evolution of the peak electrostatic fields of  $a_0 = 50, 100$  and  $150$ , from analytical model (blue solid) and one-dimensional simulations. d) Evolution of the maximum energy of background protons with  $a_0 = 50, 100$  and  $150$ , from analytical model (blue solid) and simulations. Here the dashed lines show that the peak energy increases with  $\sim t^{2/3}$ .

front foil have the peak energy below 10 GeV.

Trapping and accelerating of charged particles are determined by the velocity, amplitude and length scale of the DF structure. Since the DF co-moves with the foil, its dynamics can be derived by the momentum equation of the piston [11]

$$\frac{d(\gamma_f \beta_f)}{dt} = \frac{m_e}{m_i} \frac{2a_0^2(t-x_f)}{N_f D_f} \frac{1 - \beta_f}{1 + \beta_f}. \quad (1)$$

here  $\beta_f$  is the foil velocity normalized by  $c$ ,  $\gamma_f = (1 - \beta_f^2)^{-1/2}$ , and  $m_i$  is the ion mass.  $N_f$  and  $D_f$  are initial density and thickness of the foil normalized by the critical density  $n_c$  and laser wavelength  $\lambda_0$ . All lengths and the time are normalized by  $\lambda_0$  and  $T_0$ , respectively. The velocity of the DF structure is thus  $\beta_E = \beta_f$ , and can be obtained by solving Eq. (1).

More critical is the evolution of field amplitude. Former researches suggested that considering the balance of the electron thin layer between the light pressure and electrostatic force, the peak amplitude of the DF should be proportional to the Doppler factor  $(1 - \beta_f)/(1 + \beta_f)$  [27]. This means that it would drop by  $1/4\gamma_f^2$  in the relativistic regime. In the above simulation  $\gamma_f \approx 5$  at  $t = 500T_0$ , and the DF amplitude should decrease by some factor 100. However, as seen in Fig. 2(a) The DF at  $t = 500T_0$  is still above  $E/E_0 > 15$ , roughly one tenth of initial maximum field. A new scaling should then be

deduced. In Fig. 2(b) the distributions of laser field and electrons at  $t = 500T_0$  are presented. The laser ponderomotive force acts on only a small portion of the electrons at the surface and not on the whole electron layer. This is because the light pressure is severely weakened when the foil becomes relativistic so that it cannot confine all foil electrons. The situation is then similar to the electrostatic shock or the hole-boring process [9], except the whole system is moving fast.

Since the foil velocity varies slowly with time, it is reasonable to assume the piston frame as an inertial reference system, where relationships in Ref. [9] can be applied after Lorentz transforming all quantities. Considering the balance of the electron skin layer instead of the whole electron layer, the peak DF is  $E'_{x0} \sim \sqrt{P'_{rad}}$ , where  $P'_{rad}$  is the light pressure in the moving frame  $K'$ . The longitudinal electric field and light pressure turn out to be Lorentz invariants, thus the peak amplitude in laboratory frame is conveniently obtained by  $E_{x0} \sim \sqrt{P_{rad}} \sim \sqrt{(1 - \beta_f)/(1 + \beta_f)}$ . On the other hand, the ponderomotive force acting on electrons is approximately  $|e\beta'_e \times \mathbf{B}'_L| \approx eE'_L$ , therefore  $E'_{x0} \sim E'_L$ , giving the normalized peak amplitude of

$$E_{x0}(t) \approx a \sqrt{\frac{1 - \beta_f}{1 + \beta_f}}. \quad (2)$$

The both estimations above show that the field scales proportional to the square root of the Doppler factor, i.e., about  $1/2\gamma_f$ . This is a much weaker decay than formerly assumed. We compare the results from Eqs. (1) and (2) with 1D PIC simulation results in Fig. 2. One can see that for  $a=50, 100$  and  $150$ , Eq. 2 describes the simulation results properly. This new scaling is very important to guarantee the DF structure can be maintained for a long distance and does not vanish in relativistic regime.

The dynamics of background plasma protons encountered in the field of the piston are then derived by

$$\frac{d(\gamma_b \beta_b)}{dt} = \frac{2\pi m_e E_x(t, x_b)}{m_p}. \quad (3)$$

As seen from Fig. 1 and Fig. 2(a), the DF drops almost linearly with the distance shortly behind the foil. The long weak tail far behind the foil is neglected since protons located there are no longer trapped. We simplify the description, by assuming the charge separation field behind the skin layer decays to zero in a length scale of  $d_E$

$$E_x(t, x_b) = \begin{cases} E_{x0}(t)(1 - \frac{x_f - x_b}{d_E}), & x_f - d_E \leq x_b \leq x_f \\ 0, & elsewhere \end{cases}. \quad (4)$$

Here the  $x_b, \beta_b, \gamma_b$  are position, normalized velocity and  $\gamma$ -factor of the background protons. The scale length of

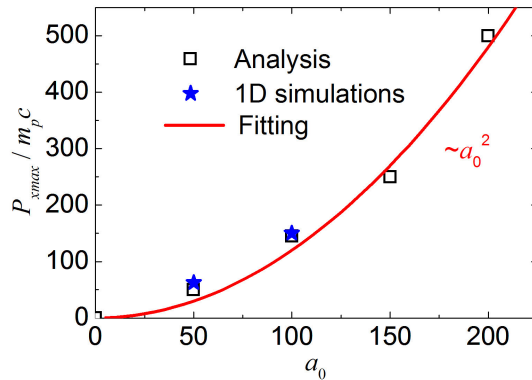


Figure 3: Scaling law of the maximum achievable momentum versus peak laser amplitude from analytical model (black square) and simulations (blue pentacle). The fitted red line indicates the power-law of  $\sim a_0^2$ .

the electrostatic field localized inside the skin layer is so small that we ignore it. Simulations suggest that the DF scale is about  $d_E \approx 40\mu\text{m}$ . Protons initially located at different positions of  $x_b|_{t=0}$ , which are also the injected positions, obtain final energy when  $x_b = x_f$ . So the maximum energy of all reflected protons as a function of time can be analytically derived by changing the  $x_b|_{t=0}$  in Eqs. (3) and (4).

Eqs. (1)-(4) offer a complete description of the mechanism. Peak momenta of the trapped protons at different simulation times and from analytical model are shown in Fig. 2(d), for  $a=50, 100$  and  $150$ , respectively. Again, the analytical results and the simulations are in a good agreement. Simulation data is also fitted, showing that the peak momentum increases with time according to the power law  $\propto t^{2/3}$ , much faster than in the simple LPA ( $\propto t^{1/3}$ ) [11]. The great difference is due to the fact that the light pressure - that drives the foil - decays as  $1/4\gamma_f^2$  while the DF accelerating the background protons decays much slower, as  $1/2\gamma_f$ . Within a few millimeters the protons are accelerated close to 100GeV, while in LPA it is nearly impossible to produce protons beyond ten GeV even in 1D simulations.

In DF acceleration, the piston is continuously accelerated. Thus, the later local protons are injected, the higher energy they obtain. However, the DF amplitude also decays meanwhile so that after certain point it becomes not intense enough to trap stationary protons. The trapping condition is obtained by balancing kinetic energy of the incoming protons and the DF electrostatic potential in the relativistic piston frame

$$\frac{1}{2}eE'_{x0}(t)d'_E = (\gamma_f - 1)m_p c^2. \quad (5)$$

where  $E'_{x0}(t) = E_{x0}(t)$  and  $d'_E = \gamma_f d_E$  is the peak amplitude and length scale of the DG field in the moving frame.

The critical foil  $\gamma$ -factor beyond which background protons are no longer trapped is then

$$\gamma_{fc} \approx 1 + \frac{\pi m_e a_0 D_E}{m_p} \quad (6)$$

For  $a_0 = 150$  and  $D_E = d_E/\lambda_0 = 40$ , the critical value is about  $\gamma_{fc} \approx 6$ . After the foil's  $\gamma$ -factor reaches the critical value, latish protons would pass through the DF structure without being trapped any more. This defines the maximum energy obtainable by this mechanism. In Fig. 3 the scaling law between the maximum obtainable energy and  $a_0$  from simulations is compared with the model. The simulation results are only shown for  $a_0 = 50$  and 100. For higher amplitudes, it would take too much time to reach the final stage (about  $10^4$  ĩijm). Fig. 3 indicates that the maximum energy is proportional to the square of the laser amplitude  $\sim a_0^2$ . This mechanism allows to accelerate protons to hundreds of GeV.

In 1D simulations we chose very low background densities to ensure that the DF is not affected. In the multi-dimensional geometry, the situation becomes more complicated. Firstly, instabilities may destroy the thin foil during the interaction. This could be restrained by using a highly relativistic laser pulse, e.g.,  $a_0 > 100$  in our case. Secondly, the foil deformation due to the laser intensity distribution will cause diffraction. Reflected parts of the laser fields interfere with each other behind the moving piston. The DF structure is well formed at the beginning, however when the perturbation arrives at the axis, it may breakdown before any protons being trapped.

To address this, we increase the background plasma density. Background electrons are snow-plowed by the driving laser and pile up inside the piston. As a result, higher background density could induce two effects. Firstly, the relativistic piston is slowed down. Secondly, the DF might be enhanced by the additional charge separating field between piled-up electrons and left-behind protons. The higher background density eases the trapping of local protons. The 2D simulation results are shown in Fig. 4. The laser pulse has the same trapezoidal profile as in 1D simulations in time domain and a super-Gaussian distribution transversely  $\sim e^{-(y/w_y)^4}$ , where  $w_y = 35\mu m$ . To restrain instabilities, the laser peak amplitude is increased to  $a_0 = 200$ . The diffraction and reflection of the incident pulse is minimized by using density matching foil, i.e., the foil is with density distribution of  $n_f(y) = n_0 e^{-(y/w_y)^4}$  [16]. The foil density and thickness are  $n_f = 80n_c$  and  $d_f = 0.62\lambda_0$  while the background plasma density is increased to  $n_b = 0.1n_c$ .

Fig. 4(a) shows distributions of the DF, electrons in the foil and background protons at  $t = 60T_0$ . It is seen that the DF is well formed behind the thin layer. Before the instabilities could develop perturbing the accelerating field, some of the background protons are trapped and accelerated. As seen in Fig. 4(b), the maximum energy of

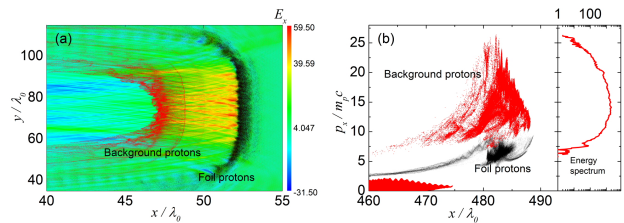


Figure 4: Two-dimensional results with  $a_0 = 200$ ,  $n_f = 80n_c$ ,  $d_f = 0.62\lambda_0$  and  $n_b = 0.1n_c$ . a) Space distributions of the foil protons (black dotted), background protons (red dotted) and the electrostatic field at  $t = 60T_0$ ; b) Momentum distributions of the foil protons (black dotted) and background protons (red dotted). The right panel is the energy spectrum of background protons.

reflected protons at  $t = 500T_0$  is about 25GeV, approximately 4 times the peak proton energy in LPA. Some foil protons left behind the layer are also trapped and accelerated to high energy. The total energy of reflected background protons is about 3% of all foil protons, which is quite considerable concerning the low background density. One would expect higher energy efficiency by using denser background plasma.

In conclusion, a method to laser accelerate protons beyond tens of GeV is proposed. It takes advantage of the electrostatic field dragging behind the flying foil in LPA to trap background protons. The dragging field keeps trapping and accelerating protons to energies greatly higher than that obtained in LPA. The analytical model shows that the electrostatic field decays more slowly than formerly assumed, resulting in larger energy increasing rate ( $\sim t^{2/3}$ ). The final maximum energy scales as  $\sim a_0^2$ . 2D simulations proved the proposal, generating protons with peak energy of about 25GeV.

This work is supported by a fellowship of the Alexander von Humboldt Foundation for Liangliang Ji, National Natural Science Foundation of China (Project No. 11125526, and No. 60921004)

- 
- [1] M. Roth et al., Phys. Rev. Lett. 86, 436 (2001).
  - [2] A. Pukhov, Phys. Rev. Lett. 86, 3562 (2001).
  - [3] S. C. Wilks et al., Phys. Plasmas 8, 542 (2001).
  - [4] R. A. Snavely et al., Phys. Rev. Lett. 85, 2945 (2000).
  - [5] P. Mora, Phys. Rev. Lett. 90, 185002 (2003).
  - [6] T. Esirkepov et al., Phys. Rev. Lett. 89, 175003 (2002).
  - [7] H. Schwöerer et al., Nature (London) 439, 445 (2006); B. M. Hegelich et al., Nature (London) 439, 441 (2006).
  - [8] S. A. Gaillard et al., Phys. Plasmas 18, 056710 (2011).
  - [9] A. Macchi et al., Phys. Rev. Lett. 94, 165003 (2005).
  - [10] B. Shen et al., Phys. Rev. E 64, 056406 (2001).
  - [11] T. Esirkepov et al., Phys. Rev. Lett. 92, 175003 (2004).
  - [12] X. Q. Yan et al., Phys. Rev. Lett. 100, 135003 (2008); B. Qiao et al., Phys. Rev. Lett. 102, 145002 (2009).

- [13] F. Pegoraro et al., Phys. Rev. Lett. 99, 065002 (2007).
- [14] X. Zhang et al., Phys. Plasmas 14, 073101 (2007); A. P. L. Robinson et al., New J. Phys. 10, 013021 (2008); O. Klimo, J. Psikal, J. Limpouch and V. T. Tikhonchuk, Phys. Rev. ST Accel. Beams 11, 031301 (2008).
- [15] A. Henig et al., Phys. Rev. Lett. 103, 045002 (2009).
- [16] M. Chen et al., Phys. Rev. Lett. 103, 024801 (2009); Tong-Pu Yu et al., Phys. Rev. Lett. 105, 065002 (2010).
- [17] J. Denavit et al., Phys. Rev. Lett. 69, 3052 (1992).
- [18] C. A. Palmer et al., Phys. Rev. Lett. 106, 014801 (2011).
- [19] D. Haberberger et al., Nature Phys. 8, 95 (2012); F. Fiuza et al., Phys. Rev. Lett 109, 215001 (2012).
- [20] L. O. Silva et al., Phys. Rev. Lett. 92, 015002 (2004).
- [21] D. W. Forslund et al., Phys. Rev. Lett. 25, 1699 (1970);
- [22] L. Romagnani et al., Phys. Rev. Lett. 101, 025004 (2008).
- [23] A. Achterberg et al., Monthly Notices of the Royal Astronomical Society 328, 393 (2001).
- [24] B. F. Shen et al., Phys. Rev. ST Accel. Beams 12, 121301 (2009); L. L. Yu et al., New J. Phys. 12, 045021 (2010); X. Zhang et al., Phys. Plasmas 17, 123102 (2010); F. L. Zheng et al., Phys. Plasmas 19, 023111 (2012).
- [25] A. Pukhov, J. Plasma Phys. 61, 425 (1999).
- [26] W. P. Wang et al., Phys. Plasmas 18, 013103 (2011)
- [27] B. Eliasson et al., New J. Phys. 11 073006 (2009); A. Macchi et al., New J. Phys. 12 045013 (2010) .